PCV

L. Teodori and H. Yik

Physics Department, University of Göttingen.

Abstract

We show what we have done to reproduce the results from [1]. We used pseudo-spectral methods to solve an extension to 2D Navier-Stokes equations that uses a piecewise constant viscosity (PCV) to model the forcing due to active agents. This PCV model allows one to regulate more precisely the strength and range of forced wavenumbers. This model shows a phase transition to the formation of vortices at the largest length scale. Also we tried an intermittent pattern forming analysis and characterize the range of the parameters for which this can happen in our model.

FIG. I.1: Remarkable demonstration of polar order in a sardine school

I. ACTIVE FLUIDS

An active fluid [2] is a densely packed soft material whose constituent elements can self-propel. Examples include dense suspensions of bacteria, microtubule networks or artificial swimmers (see figures I.2 and I.1).

The interaction of active particles with each other, and with the medium they live in, gives rise to highly correlated collective motion and mechanical stress. A distinctive, indeed, defining feature of active systems compared to more familiar nonequilibrium systems is the fact that the energy input that drives the system out of equilibrium is local, for example, at the level of each particle, rather than at the system's boundaries as in a shear flow.

II. SOLVING NUMERICALLY NAVIER STOKES

We used ω- ψ formalism, so from the incompressible Navier Stokes,

$$\frac{\partial \mathbf{u}}{\partial t} + \mathbf{u} \cdot \nabla \mathbf{u} = -\frac{\boldsymbol{\nabla} P}{\rho} + \nu \nabla^2 \mathbf{u} \ , \tag{II.1}$$

apply the curl on both sides to reduce to an equation for the vorticity $\boldsymbol{\omega} = \boldsymbol{\nabla} \times \mathbf{u}$ (recalling that for incompressible flows $\boldsymbol{\nabla} \cdot \mathbf{u} = 0$)

$$\frac{\partial \boldsymbol{\omega}}{\partial t} + (\boldsymbol{\nabla} u_i) \times \partial_i \mathbf{u} + u_i \partial_i \boldsymbol{\omega} = \nu \nabla^2 \boldsymbol{\omega} \ . \tag{II.2}$$

In 2 dimensions, one has that the curl is defined as

$$\boldsymbol{\nabla} \times (u_x \hat{\mathbf{x}} + u_y \hat{\mathbf{y}}) \equiv (\partial_x u_y - \partial_y u_x) \hat{\mathbf{z}} \ . \tag{II.3}$$

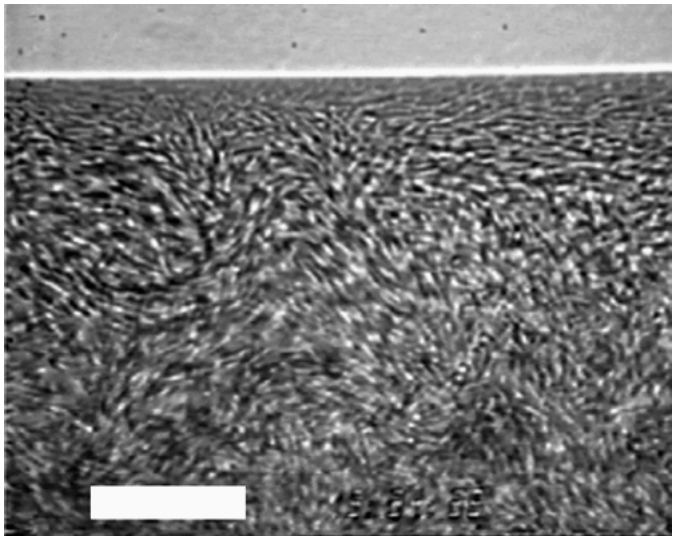

FIG. I.2: Bacterial "turbulence" in a sessile drop of Bacillus sub-tilis viewed from below through the bottom of a petri dish. Gravity is perpendicular to the plane of the picture, and the horizontal white line near the top is the air-water-plastic contact line. The central fuzziness is due to collective motion. The scale bar is 35 μm.

We can consider the vorticity as a scalar function (I need only one scalar component to fully describe it) and also we have

$$(\boldsymbol{\nabla} u_i) \times \partial_i \mathbf{u} = (\boldsymbol{\nabla} \cdot \mathbf{u})(\boldsymbol{\nabla} \times \mathbf{u}) = 0 \tag{II.4}$$

where on the last step we used incompressibility. So the final equation is

$$\partial_t \omega + \partial_y \psi \partial_x \omega - \partial_x \psi \partial_y \omega = \nu \nabla^2 \omega \ , \tag{II.5}$$

where we have used the so called stream function

$$\frac{\partial \psi}{\partial y} = u_x \ , \quad \frac{\partial \psi}{\partial x} = -u_y \implies \omega = -\nabla^2 \psi \ . \tag{II.6}$$

In Fourier space this becomes

$$\partial_t \hat{\omega} = -i(k_x \widehat{u_x \omega} + k_y \widehat{u_y \omega}) - \nu k^2 \hat{\omega} \ , \quad \hat{\psi} = \hat{\omega}/k^2 \ . \tag{II.7}$$

To treat numerically the non linearity, we can use pseudo spectral methods. The idea is to solve the spatial part of the equation in Fourier space trying to avoid to directly Fourier transform the non-linear term (which would involve a convolution, a heavy process from the computational point of view) but rather perform the multiplication in real space. Then the

time evolution is performed numerically. In formulas, calling $N \equiv -i(k_x\widehat{u_x\omega} + k_y\widehat{u_y\omega})$ the non linearity,

$$\hat{N} = -ik_x\mathcal{F}(\mathcal{F}^{-1}(\hat{u}_x)\cdot\mathcal{F}^{-1}(\hat{\omega})) - ik_y\mathcal{F}(\mathcal{F}^{-1}(\hat{u}_y)\cdot\mathcal{F}^{-1}(\hat{\omega}))\ . \tag{II.8}$$

Going back and forth from real space to the Fourier one is way better than doing the convolution since fast Fourier transform algorithms (FFT) can perform the Fourier transform in $\mathcal{O}(N\log N)$ steps rather than $\mathcal{O}(N^2)$.

Since the problem in Navier-Stokes is only the non linearity, we can implement the integrating factor method to exactly solve the linear part and applying numerical methods for the non linear part, so write

$$\partial_t(e^{\nu k^2 t}\hat{\omega}) = e^{\nu k^2 t}\hat{N}\ , \tag{II.9}$$

such that the exact linear solution is encoded on the exponential factor. Then apply explicit second order Runge-Kutta to evolve it in time,

$$\begin{aligned}\hat{\omega}^* =& e^{-\nu k^2\delta t/2}\Big(\hat{\omega}(t) + 0.5\delta t\hat{N}(\hat{\omega}(t))\Big)\ ,\\ \hat{\omega}(t+\delta t) =& e^{-\nu k^2\delta t/2}\Big(e^{-\nu k^2\delta t/2}\hat{\omega}(t) + \delta t\hat{N}(\hat{\omega^*})\Big)\ .\end{aligned} \tag{II.10}$$

III. ACTIVE SUSPENSIONS

An active suspension is, roughly speaking, a passive fluid medium that contains at least one "micro-swimmer" species capable of converting chemical into kinetic energy. If the swimmer concentration is sufficiently high, their collective dynamics can induce rich non-equilibrium flow patterns in the ambient fluid. In dense bacterial suspensions, the mean bacterial velocity field $u(t,x)$, which can be approximately decomposed in the form $u(t,x) = v + v_0P$ where v is the underlying solvent velocity field and P denotes the local mean orientation of the bacteria. The parameter v_0 is the typical bacterial self-swimming speed relative to the solvent flow (in general, v_0 is also a fluctuating quantity). Aiming to develop a simplified phenomenological framework for the future mathematical description of rheological measurements, we will focus here on the complementary problem of constructing effective models for the solvent velocity field.

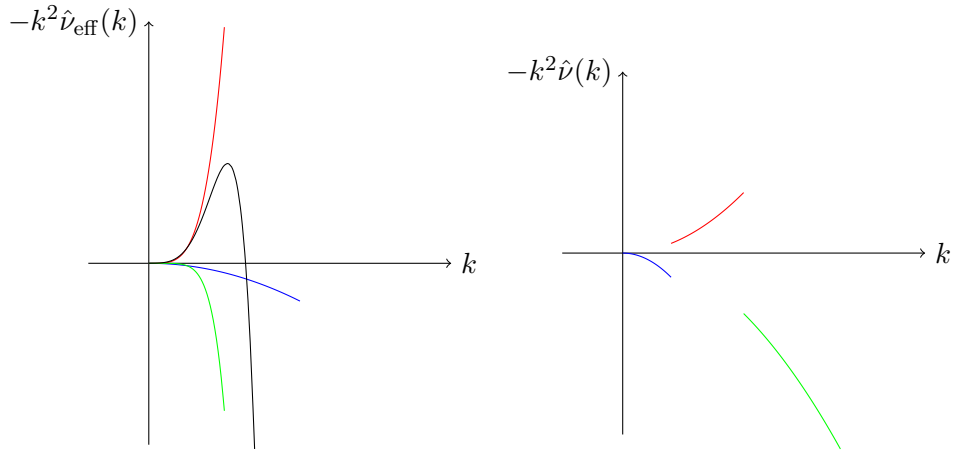

FIG. IV.1: On the left, the behavior of $\nu_{\text{eff}}k^2$ for the generalized Navier-Stokes model and on the left the same for the PCV model.

IV. PCV MODEL

A typical extension to Navier-Stokes equations [3] is

$$\partial_t \mathbf{u} + (\mathbf{u}\cdot\nabla)\mathbf{u} + \boldsymbol{\nabla} P = \boldsymbol{\nabla}\cdot\sigma \ , \tag{IV.1}$$

with

$$\sigma_{ij} = (\Gamma_0 - \Gamma_2\nabla^2 + \Gamma_4(\nabla^2)^2)(\partial_i u_j + \partial_j u_i) \ . \tag{IV.2}$$

The action of the modified stress tensor σ_{ij} can be resumed in an effective viscosity coefficient

$$\partial_t \hat{\mathbf{u}} + \mathcal{F}((\mathbf{u}\cdot\nabla)\mathbf{u}) - i\mathbf{k}\hat{P} = -k^2\nu_{\text{eff}}(k)\hat{\mathbf{u}} \ .$$

In figure IV.1, we put the plots of ν_{eff} for the generalized Navier-Stokes model and PCV model. In the various colors, we represented:

- Effective viscosity $\quad \hat{\nu}_{\text{eff}}(k) = \Gamma_0 + \Gamma_2 k^2 + \Gamma_4 k^4$;
- $\Gamma_0 \iff$ kinematic viscosity;
- $\Gamma_2 < 0$ determines both strength and range of forced wave numbers.
- $\Gamma_4 > 0 \iff$ damping of large k modes by hyperviscosity;

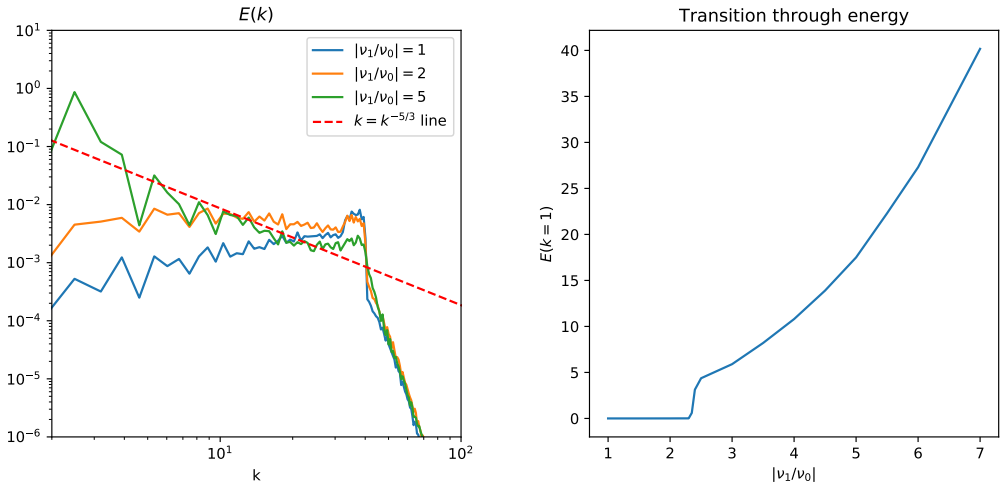

FIG. V.1: On the left, energy dispersion relation for three different values of $|\nu_1/\nu_0|$; on the right, we see the transition from small scale structure formation to large scale ones at a value of $|\nu_1/\nu_0| = 2.3$.

V. PCV MODEL

To model more precisely the forcing of wave numbers due to bacteria, introduce a piecewise constant viscosity (PCV) [1]:

$$\hat{\nu}(k) = \begin{cases} \nu_0 > 0 & \text{for} \quad k < k_{\min} \ , \\ \nu_1 < 0 & \text{for} \quad k_{\min} \leq k \leq k_{\max} \ , \\ \nu_2 > 0 & \text{for} \quad k > k_{\max} \ ; \end{cases}$$

so that the equation to solve is

$$\partial_t \hat{\omega} - \hat{N} = -\hat{\nu}(k) k^2 \hat{\omega} \ .$$

To numerically solve it, we used the same method we described for Navier-Stokes equations.

We managed to reproduce the main results of [1], see figure V.1; this was helpful in trying to validate our code.

A. Technical details

a. Stability. Since we used an explicit method, we had to use an adaptive time step using Courant-Friedrichs-Lewy (CFL) time condition, that is

$$\delta t = \frac{\Delta x}{u_{\max}} = \frac{L}{N u_{\max}} \ , \tag{V.1}$$

where L is the length of the grid, N the grid spacing and $u_{\max}$ the modulus of the maximum velocity.

b. Aliasing. As noted in [4], in order to prevent aliasing we put the modes with $k \geq 2k_{\max}/3$ to zero always before a non-linear evaluation.

B. Scaling relations

We saw that scaling $\nu(k)$ does not change the pattern followed by the solution $\mathbf{u}$; in fact, non dimensionalizing our Navier Stokes equation extension using

$$u = Uu' \ , \quad x = Lx' \implies t = \frac{L}{U}t' \ , \quad k = \frac{1}{L}k' \ , \quad \omega = \frac{U}{L}\omega' \ , \tag{V.2}$$

we have

$$\partial_{t'}\hat{\omega'} - \hat{N'} = -\frac{\hat{\nu}(k)}{UL}k'^2\hat{\omega'} \ , \tag{V.3}$$

where on the RHS we have the Reynolds number $R_e = UL/\hat{\nu}(k)$. Since the space grid is never changed in our simulations, we expect that the only variable upon scaling of ν is the typical velocity; increasing the viscosity means that the velocity is greater, and if indeed we have that

$$\nu \to \lambda\nu \implies u \to \lambda u \ , \tag{V.4}$$

we can conclude that the Reynolds number remains the same, meaning indeed that the pattern of the fluids with according scaled variables is the same if (V.4) holds.

In the end we thus fixed a scale for ν by fixing ν_0 and analyzed the range of parameters resumed in table V.1 (the only free parameter is then ν_1).

VI. INTERMITTENT PATTERN ANALYSIS

We tried to see and analyze intermittent pattern forming, that is pattern formation arising when forcing only one mode. In general, patterns initially form but then, due to non

N	ν_0	ν_1/ν_0	ν_2/ν_0	$k_{\min}$	$k_{\max}$
256	10^{-4}	-0.25-(-7.0)	10	33	40

TABLE V.1: Parameters used in our analysis.

linearities, the pattern changes [5].

In figure VI.1, we see the various patterns forming for different forcing wavenumbers; we see that the magnitude of k sets the scale of patterns, and also we see that a same pattern can appear for different values of k. The interesting thing is that different patterns can form and disrupt during the same simulation.

In figure VI.2, we see what characterize a pattern-forming system.

In figure VI.3, we can see how one can easily build a criterion for distinguishing pattern forming systems from non-pattern forming one by looking at the behavior of $E(k)$.

In figure VI.4 we present the main result of our work, that is the parameter range where you have intermittent pattern forming systems (which are the ones with the higher E_{forcing}/E ratio).

VII. CONCLUSIONS

PCV model enables an easy control of forcing/dissipation, so that one can have a large spanning of possible models with control of few parameters. We exploited the PCV features to study of intermitting pattern states, since we can have a direct control of forced wavenumbers.

Future works in this respect can include a more in depth analysis of parameters giving intermittent patterns and a statistical analysis of appearance of specific patterns.

The python code used for this work is available here.

[1] M. Linkmann, G. Boffetta, M. Marchetti, and B. Eckhardt, (2018).

[2] M. C. M. et al, Reviews of Modern Physics (2013).

[3] J. Słomka and J. Dunkel, The European Physical Journal (2015).

[4] S. A. Orszag, Journal of the Atmospheric Science (1971).

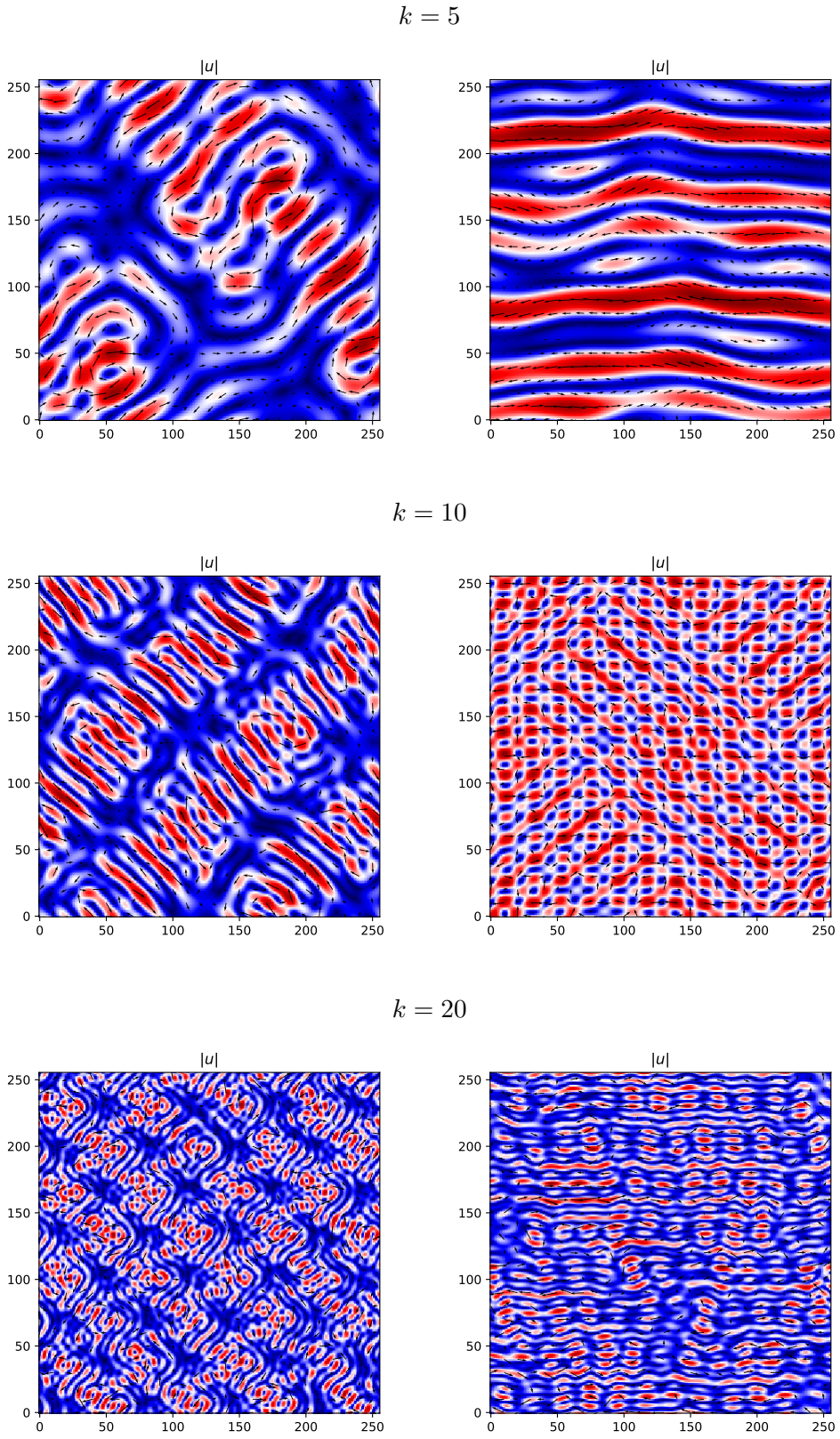

FIG. VI.1: Snapshots of different patterns corresponding to different forcing scales.

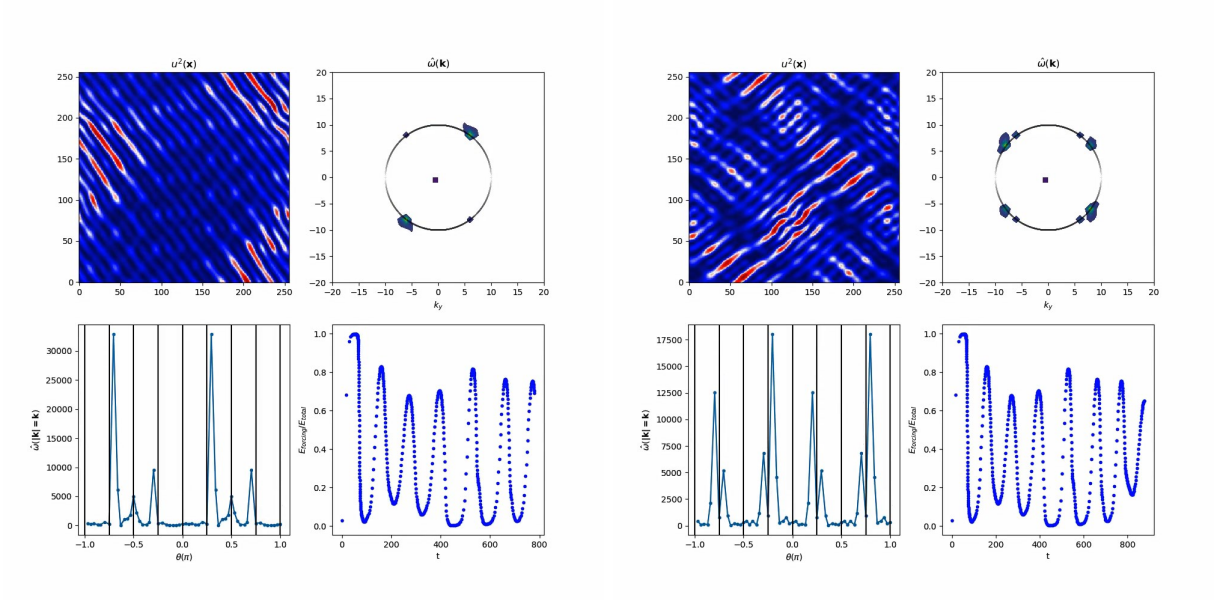

FIG. VI.2: Plots characterizing pattern forming systems.

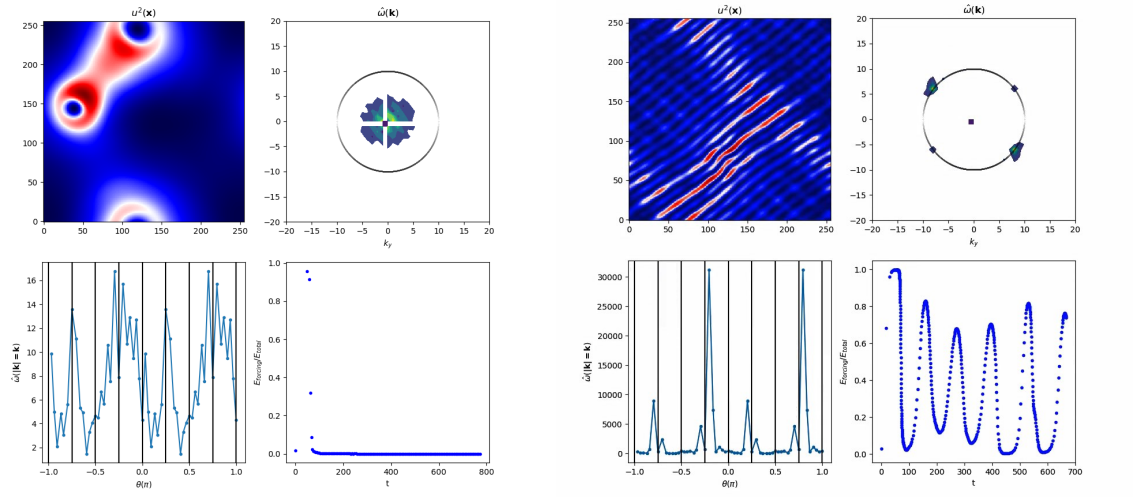

FIG. VI.3: Example of pattern forming system on the right and a not pattern forming one on the left.

[5] O. Mickelin and J. S. et al, Physical Review Letters (2018).

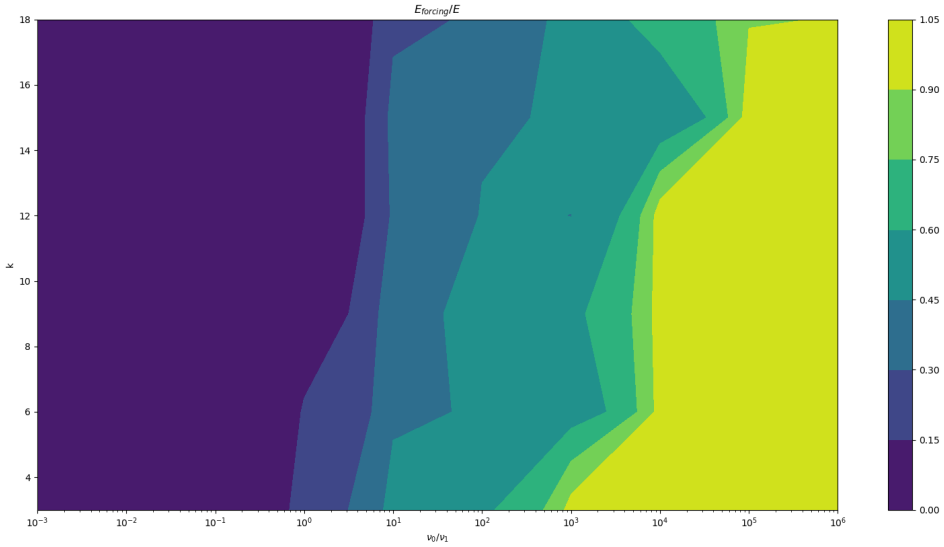

FIG. VI.4: Intermittent pattern phase diagram.